NeuroImage: Clinical 4 (2014) 426–435

Contents lists available at ScienceDirect

NeuroImage: Clinical

journal homepage: www.elsevier.com/locate/ynicl

Application of quantitative DTI metrics in sporadic CJD ☆

E. Caverzasi [a,b,*,1,2], R.G. Henry [a,c,d,1,3], P. Vitali [e,1,4], I.V. Lobach [a,5], J. Kornak [f,6,7], S. Bastianello [b,1,8], S.J. DeArmond [g,h,9,10], B.L. Miller [i,11,12], H.J. Rosen [i,1,13], M.L. Mandelli [i,1,14], M.D. Geschwind [i,3,15]

[a] Department of Neurology, University of California, San Francisco (UCSF), San Francisco, CA, USA
[b] Department of Neuroradiology, C. Mondino National Neurological Institute, Pavia. University of Pavia, Italy
[c] Graduate Group in Bioengineering, UCSF, San Francisco, CA, USA
[d] Department of Radiology and Biomedical Imaging, UCSF, San Francisco, CA, USA
[e] Brain MRI 3T Mondino Research Center C. Mondino National Neurological Institute, Pavia, Italy
[f] Department of Epidemiology and Biostatistics, UCSF, San Francisco, CA, USA
[g] Institute for Neurodegenerative Diseases, University of California, San Francisco (UCSF), USA
[h] Department of Pathology, University of California, San Francisco (UCSF), USA
[i] Memory and Aging Center, Department of Neurology, University of California, San Francisco, (UCSF), USA

ARTICLE INFO

Article history:
Received 18 October 2013
Received in revised form 13 December 2013
Accepted 17 January 2014
Available online 31 January 2014

Keywords:
Creutzfeldt–Jakob disease
Prion disease
Atrophy
DWI
sCJD
MD

ABSTRACT

Diffusion Weighted Imaging is extremely important for the diagnosis of probable sporadic Jakob–Creutzfeldt disease, the most common human prion disease. Although visual assessment of DWI MRI is critical diagnostically, a more objective, quantifiable approach might more precisely identify the precise pattern of brain involvement. Furthermore, a quantitative, systematic tracking of MRI changes occurring over time might provide insights regarding the underlying histopathological mechanisms of human prion disease and provide information useful for clinical trials. The purposes of this study were: 1) to describe quantitatively the average cross-sectional pattern of reduced mean diffusivity, fractional anisotropy, atrophy and T1 relaxation in the gray matter (GM) in sporadic Jakob–Creutzfeldt disease, 2) to study changes in mean diffusivity and atrophy over time and 3) to explore their relationship with clinical scales. Twenty-six sporadic Jakob–Creutzfeldt disease and nine control subjects had MRIs on the same scanner; seven sCJD subjects had a second scan after approximately two months. Cortical and subcortical gray matter regions were parcellated with Freesurfer. Average cortical thickness (or subcortical volume), T1-relaxiation and mean diffusivity from co-registered diffusion maps were calculated in each region for each subject. Quantitatively on cross-sectional analysis, certain brain regions were preferentially affected by reduced mean diffusivity (parietal, temporal lobes, posterior cingulate, thalamus and deep nuclei), but with relative sparing of the frontal and occipital lobes. Serial imaging, surprisingly showed that mean diffusivity did not have a linear or unidirectional reduction over time, but tended to decrease initially and then reverse

☆ This work was supported by NIH/NIA R01 AG-031189, K23 AG021989, P50AG023501, NIH/NCRR Grant Number UL1 RR024131, NIH/NIA AG021601, and NIH/NINDS Contract N01-NS-0-2328.

* Corresponding author at: Box 3206, University of California, San Francisco, San Francisco, CA 94143, USA. Tel.: +1 415 476 2900; fax: +1 415 476 2921.
E-mail address: ecaverzasi@gmail.com (E. Caverzasi).

[1] Nothing to disclose related to this paper.
[2] Study concept and design, acquisition of data, analysis and interpretation, critical revision of the manuscript for important intellectual content.
[3] Study concept and design, acquisition of data, analysis and interpretation, critical revision of the manuscript for important intellectual content, study supervision.
[4] Study concept and design, acquisition of data, critical revision of the manuscript for important intellectual content.
[5] Statistical analysis, interpretation, critical revision of the manuscript for important intellectual content.
[6] Paid a consulting fee by UCSF CTSI consulting for manuscript statistical analysis.
[7] Analysis and interpretation (statistical analysis).
[8] Critical revision of the manuscript for important intellectual content.
[9] Funded by the NIH (AG021601).
[10] Analysis and interpretation.
[11] Receives grant support from the NIH/NIA and has nothing to disclose related to this paper. Dr. Miller serves as a consultant for TauRx, Allon Therapeutics, Lilly USA LLC and Siemens Medical Solutions. He has also received a research grant from Novartis. He is on the Board of Directors for the John Douglas French Foundation for Alzheimer's Research and for The Larry L. Hillblom Foundation.
[12] Critical revision of the manuscript for important intellectual content, study supervision.
[13] Study supervision, critical revision of the manuscript for important intellectual content.
[14] Analysis and interpretation, critical revision of the manuscript for important intellectual content.
[15] Funded by the NIH/NIA R01 AG-031189, NIH/NIA K23 AG021989; NIH/NIA AG031220 and Michael J. Homer Family Fund. Dr. Geschwind has served as a consultant for Lundbeck Inc., MedaCorp, The Council of Advisors, and Neurophage.

http://dx.doi.org/10.1016/j.nicl.2014.01.011

and increase towards normalization. Furthermore, there was a strong correlation between worsening of patient clinical function (based on modified Barthel score) and increasing mean diffusivity.

1. Introduction

Sporadic Jakob–Creutzfeldt disease (sCJD) is unique among neurodegenerative diseases as there is an MRI marker (restricted diffusion of certain gray matter regions) with very high sensitivity and specificity (Meissner et al., 2009; Vitali et al., 2011; Young et al., 2005). Most prior MRI studies in sCJD studying cortical restricted diffusion have been performed by a visual assessment analysis on fluid-attenuated inversion recovery (FLAIR) and/or diffusion weighted images (DWI) sequences (Meissner et al., 2009; Tschampa et al., 2007; Vitali et al., 2011; Young et al., 2005). Due to MRI susceptibility and other artifacts, this "qualitative" approach, however, may not show the extent of true brain involvement (Lin et al., 2006). Improved understanding of the quantification and pattern of brain MRI changes that occur in sCJD (such as atrophy and diffusion) (Cohen et al., 2009; Lee et al., 2012; Wang et al., 2013) as well as their changes over time might provide important biomarker data to track for future clinical trials, as well as provide insights on mechanisms of the disease and prion spread. Tracking MRI progression in other neurodegenerative diseases has usually been done by following structural measures of white or gray matter integrity or metabolism; such studies have consistently reported a roughly linear or unidirectional decline (Driscoll et al., 2009; Shiga et al., 2004). Additionally, it is not clear what happens with restricted diffusion over time in sCJD (Geschwind et al., 2009; White et al., 2003). To our knowledge, there have been no formal studies on the course of DWI overtime in human prion disease, only case reports. Some case reports suggest increasing DWI involvement (Kono et al., 2011; Ukisu et al., 2005), whereas others suggest less DWI involvement, particularly with atrophy (Matoba et al., 2001; Tribl et al., 2002).

Although diffusion tensor imaging (DTI) has emerged as a sensitive diagnostic technique highlighting mean diffusivity (MD) abnormalities in the gray matter (GM) in human prion diseases, few studies quantified MD and fractional anisotropy (FA) abnormalities and none have examined regional and whole brain MD and FA both cross-sectionally and longitudinally in a cohort of sCJD patients (Andrews, 2010; Fulbright et al., 2006; Manners et al., 2009; Ukisu et al., 2005; Wang et al., 2013). Our aims were 1) to describe quantitatively the average pattern of reduced MD, FA, atrophy and T1 relaxation in the gray matter (GM) in sCJD as well as 2) to determine the changes of mean diffusivity and atrophy over time and 3) their relationship with clinical scales in a sub-cohort with serial imaging.

2. Material and methods

2.1. Subjects

All subjects or their designees provided informed consent for participation in this study, which was approved by our institutional review board. Subjects were evaluated between August 2005 and August 2008 at the University of California of San Francisco (UCSF) Memory and Aging Center. We analyzed all serial sCJD subjects who had the same MRI protocol of adequate quality MRI (n = 26; mean age 62, SD ±9; 46% female). Twenty-three of 26 sCJD subjects (88%) had brain autopsy and were ultimately pathologically-proven sCJD (Table 1) (Kretzschmar et al., 1996); the three other subjects eventually met UCSF 2007 (Geschwind et al., 2007) and either WHO, 1998 or European probable sCJD criteria (WHO, 1998; Zerr et al., 2009). MRIs from nine healthy age and gender matched subjects were used as controls (mean age 62 (SD ±16) 44% female). Seven sCJD subjects had a second, serial brain MRI after about two months (2.17, SD ±0.23 months).

All sCJD subjects had a Mini-Mental State examination (MMSE), the modified Barthel index, the Neuropsychiatric Inventory total score (NPI; to assess the behavioral impairments) (Cummings, 1997) and detailed standardized neurological examination (±3 days from MRI scan date) (See Supplemental data and Table 1). For cases with pathology, prion typing was performed by the National Prion Disease Pathology Surveillance Center (NPDPSC; Cleveland, OH). Prion gene, *PRNP*, analysis for mutations and codon 129 polymorphisms done through the NPDPSC. All but one sCJD subjects were tested for *PRNP* mutations; this subject was not pathologically-proven, but had no family history of neuropsychiatric disorder and presented clinically as sCJD.

2.2. Imaging acquisition

Images were acquired on a 1.5 T GE Signa scanner. The acquisition protocol consisted in two axial T1-weighted 3D IRSPGR (axial slab with 60 slices of 3 mm thickness, TR/TE = 27/6 ms, in-plane matrix 256 × 256 covering a FOV of 24 × 24 cm^2 flip angle 40° and 8°), an axial T2 FLAIR (48 slices of 3 mm thickness, TR/TE/TI = 8802/122/2200 ms, 512 × 512 matrix with a FOV of 24 × 24 cm^2), and a DTI acquisition (15 non-collinear gradient directions with b = 1000 s/mm^2, one b = 0 reference image, 35 contiguous slices of 3 mm thickness, TR/TE = 12,400/69 ms, 128 × 128 matrix covering a FOV of 25.6 × 25.6 interpolated to give a final 1 × 1 × 3 mm^3 resolution). Due to acquisition windowing problems, information on the inferior temporal lobe (entorhinal, fusiform, inferiotemporal, middletemporal, temporal pole ROIs) was lost for three subjects.

2.3. Imaging analysis

The two T1-weighted 3-D inversion recovery-spoiled images (40 and 8°) were used to calculate the T1 relaxometry maps (T1R). FreeSurfer Image Analysis Suite 4.5 version (http://surfer.nmr.mgh.harvard.edu/) (Dale et al., 1999; Fischl et al., 1999) was used for cortical reconstruction, volumetric segmentation, subcortical (Fischl et al., 2004) and cortical parcellation (Desikan-Kyliany Atlas: 40 VOIs per hemisphere with Freesurfer Atlas), as well as determining cortical thickness in each VOI and deep nuclei volumes. Volumes were normalized for intracranial volume (Desikan et al., 2006). Segmentation results were assessed by an experienced operator to ensure accuracy.

Mean diffusivity and fractional anisotropy (FA) maps were calculated after eddy current and head motion correction. DTI data were corrected by applying an affine alignment of each image to the first no diffusion weighted (b0) image using the Oxford FSL toolkit (http://www.fmrib.ox.ac.uk/fsl/fdt/index.html). DTI maps were registered to the T1-weighted images. To decrease the potential effect of partial volume averaging, the Freesurfer mask of CSF was applied to exclude voxels that were likely to contain a mixture of CSF with GM from the VOI boundary. Averages were calculated for MD, FA, T1R, and thickness or volume for each VOI.

2.4. Statistical analysis

2.4.1. Cross-sectional analysis

Age-corrected Z-scores were used in the Mann–Whitney *U* test to compare the differences between the subjects and controls for MD, FA, T1R, cortical thickness and subcortical volumes (volumes corrected for intracranial volume). The Spearman non-parametric test was used to assess the correlation between the diffusion and volumetric parameters and the clinical data of the patients, as well as correlation test between MD and thickness Z-scores. False discovery rate (FDR) adjustment was

Table 1
Summary of healthy control and sCJD cohort of demographics.

Group	N	Sex	Age (mean)	MMSE (mean, median, range)	Barthel (mean, median, range)	NPI (mean, range)	Mean time between symptoms outbreak and MRI (months)	Total mean disease duration (months)	Mean time ratio[a]	% path-proven	Codon 129[b]	Molecular Classification	
Healthy controls	9	4F (44%); 5M (56%)	61 ± 16 [c]	–	–	–	–	–	–	–	–	–	
sCJD	26	12F (46%); 14M (54%)	62 ± 9	13 ± 9 16 (0–25)	61 ± 32 78 (5–100)	29 ± 22 22 (4–87)	12 ± 8	19 ± 13	0.6 ± 0.1	88%	MM 58%[d] MV 31% VV 8% N/A 4%	MM1 MM2 MM 1/2 MM N/A MV1 MV2 MV 1/2 MV N/A VV2 N/A	15% 23% 12% 8% 8% 15% 4% 4% 8% 4%

"–" = not relevant. N/A = data not available. M = methionine. V = valine.
[a] Time ratio is ratio of time from disease onset to MRI/total disease duration.
[b] All but one sCJD subjects ruled out for gPrD by PRNP analysis; this subject was not path-proven, but had no family history of neuropsychiatric disorder and presented clinically like sCJD.
[c] ± refers to standard deviation (SD).
[d] One subject with codon 129 data, but no Western blot prion typing available, was called MM 1 based on the histopathology autopsy findings. Percentages might not add exactly due to rounding.

applied to correct for multiple comparisons. Differences in the degree of pathology measured by MD were examined across molecular subtype groups in terms of prion type and codon 129. Specifically, logistic regression analyses were performed to investigate differences in MD Z-scores across groups at the lobar level based on prion type or codon 129 polymorphism; smaller ROIs were not evaluated due to concern for reduced statistical power. Both main effects of MD Z-scores and effects of MD Z-Scores adjusted for modified Barthel Scores were examined; the latter to adjust for potential confounding due to differences in the disease stage. These effects are reported in terms of t-statistic values corresponding to Odds Ratio estimates.

2.4.2. Longitudinal analysis

The nonparametric Wilcoxon signed rank test was used to evaluate differences between the first and second time MRI points, with FDR adjustment to correct for multiple comparisons. The nonparametric Wilcoxon rank sum test was used to compare clinical scale scores and time periods between the seven serial subjects and the 19 subjects with a single scan.

Spearman correlation coefficients were used to assess the correlation between the longitudinal changes ("delta scores") of either MD, FA or thickness/volume vs. delta scores of clinical scales (e.g., MMSE, Barthel and NPI). FDR adjustment was used to correct for multiple comparisons only for VOIs; for lobar or hemispheric analyses no correction was performed.

2.4.3. Cross-sectional and longitudinal smoothing splines

Smoothing Splines were applied to examine non-linearities in the following two relationships: a) cross-sectional average GM MD or thickness/volume vs. Barthel scores; b) two-month changes in GM MD vs. Barthel score at the baseline. Smoothing Splines were applied to investigate an average tendency among behaviors of the whole brain; occipital, frontal, temporal, parietal lobes, limbic structure. Accuracy an estimate of the average tendency is examined based on 1000 bootstrap samples and presented using 95% confidence intervals. The analysis was performed using R Package for Scientific Computing (Efron and Tibshirani, 1993; Green and Silverman, 1994; R Core Team, 2013).

3. Results

The distribution of our codon 129 polymorphism subtypes in our cohort was somewhat different than that expected for an sCJD population (Chi-Square, $P < 0.001$), with both MV and VV over-represented and fewer MM than expected (Table e1) (Alperovitch et al., 1999). We could not compare the distribution of our full molecular subtypes to those expected for sCJD (Parchi et al., 1999) as they have not yet been established for Type 1/2 (Cali et al., 2009), which we had in our population. The cohort was moderately advanced cognitively with a median MMSE of 16/30, but only mildly functionally impaired with a median Barthel of 78/100 (Table 1).

3.1. Cross-sectional analysis

3.1.1. Cortical GM DTI metrics

With FDR, there was statistically significant MD reduction in several VOIs of parietal, temporal and occipital lobes, whereas in the frontal and limbic lobes only in the right medial orbitofrontal (frontal), and bilaterally in the isthmus cingulate and right posterior cingulate (limbic) (Table 2; Fig. 1). There also was a more widespread trend towards reduction of average MD in the cortical GM of sCJD compared to controls particularly within frontal lobes (Fig. 1). No increased diffusion was identified in any sCJD VOI. Sporadic CJD patients did not show any statistical significant FA change compared to controls.

3.1.2. Subcortical GM DTI metrics

With FDR, there was statistically significant MD reduction in the sCJD group compared to controls bilaterally in the caudate, putamen, thalamus, and pallidum and left amygdala (Table 2; Fig. 1). The right amygdala showed only a trend towards MD reduction (Fig. 1). Sporadic CJD patients did not show any statistical significant FA change compared to controls.

3.1.3. Comparison of GM lobar MD findings based on prion type or codon 129 polymorphism

The average lobar MD was significantly lower in subjects with type 1 compared to type 2 PrP^{Sc} bilaterally in the occipital and parietal lobes, and in the right limbic and right temporal lobes ($p < 0.05$). There were an insufficient number of subjects to analyze further by complete molecular subtype (Parchi et al., 1999) or by those with types 1 and 2 PrP^{Sc} (Cali et al., 2009). There were no differences in average lobar MD by codon 129 polymorphism. Using regression analysis accounting for Barthel scores, confirmed the main effect of the prion type on MD differences (average MD in type 1 < type 2), specifically bilaterally in the parietal (left $p = 0.048$, $t = 1.8$; right $p = 0.02$, $t = 1.3$) and occipital lobes (left $p = 0.04$ $t = 1.8$; right $p = 0.01$, $t = 2.4$) and in the right limbic ($p = 0.02$, $t = 2.2$) and right temporal ($p = 0.03$, $t = 2$), lobes. Correcting for Barthel score in a regression analysis showed an effect of the codon 129 polymorphism (MM, MV, and VV) on MD. MM cases had reduced average MD than VV cases in left temporal ($p = 0.02$, $t = 2.08$) lobe, whereas VV cases had reduced average MD in the deep nuclei (left $p = 0.03$, $t = -2.0$; right $p = 0.04$, $t = -1.8$).

3.1.4. Cortical GM subcortical GM thickness/volume and T1R

With FDR, there were no statistically significant differences in cortical thickness or volume in the sCJD group compared to controls. In the Supplemental data, we report the results without FDR correction (Supplemental data). No statistically significant T1R value differences were found between sCJD and controls in any VOIs, including the globus pallidus (GP), either with or without FDR (not shown).

3.1.5. Correlations between gray matter values and clinical scales and times/duration

There were no significant correlations, or even trends, between clinical scales and cross-sectional GM MD values, GM thickness/volume in any VOI, lobar and whole brain based analysis (not shown). There was no correlation, or even trends, of MD values with thickness or volumes in any of the cortical or subcortical GM VOIs, lobar and whole brain based analysis (not shown). No correlations or trends were found between GM MD or GM thickness (or volume) values in any VOI, lobar and whole brain based analysis with time to MRI, the total disease duration or the MRI/duration ratio (not shown).

3.2. Longitudinal analysis

The subset of seven subjects analyzed longitudinally (1 MV2, 3 MM2, 1 MM1, 1 MM 1/2 and 1 MM N/A) did not differ significantly (nonparametric Wilcoxon rank sum test) in MMSE ($p = 0.6$), NPI ($p = 0.45$) disease duration ($p = 0.24$), and time to MRI ($p = 0.86$) from the 19 subjects with MRI at a single time point. The disease ratio (time to first MRI/disease duration), however, was statistically significant smaller in the seven longitudinal than in the 19 subjects with a single MRI (cross-sectional only) (0.51 +/− 1.7 versus 0.74 +/− 1.5; $p = 0.007$ $z = -2.7$), suggesting that the seven serial subjects were temporally earlier in their disease course. The modified Barthel ($p = 0.15$) trended towards being worse in the 19 cross-sectional only subjects. Curiously, the four patients with high baseline Barthels (100–80) had a much smaller mean decline in Barthel (Mean −1.25 +/− 2.5 SD) compared to the three patients with lower baseline Barthels (range, 75–35) who had a greater average decline in Barthel (Mean −20 +/− 13 SD) over the two month interval.

3.2.1. Delta GM DTI metrics and relationship with delta clinical scales

Over approximately two-months, in seven serial sCJD subjects, most VOIs had increasing average MD from baseline, although a few VOIs continued to show reducing MD from baseline; none of these serial changes, however, were statistically significant, either with or without FDR (Supplemental Fig. 1). There were no any statistical significant longitudinal FA changes.

Regarding the relationship of change in GM MD and clinical scales, surprisingly at the whole brain, hemispheric, and lobar level, all areas showed an inverse relationship between delta Barthel and delta MD over two months—as Barthel decreased/worsened, MD increased (Supplemental Table 1). At the VOI level, 15 of 80 VOIs also reached statistical significance with FDR showing an inverse relationship between delta Barthel and delta MD (Fig. 2 and Supplemental Table 1). No correlations were found between delta MD and delta MMSE or NPI at VOI, lobar, hemisphere or whole brain cortical or subcortical GM level (data not shown).

3.3. MD as function of Barthel score in cross-sectional and longitudinal analyses

The relationship between Barthel score and both MD values (Figs. 3A–B: cross-sectional) and MD changes (Figs. 3C–D: longitudinal) seems to follow a quadric fit within a window of Barthel 100 to approximately 70. Within this window, MD values seem to follow two different phases: Phase 1. MD follows a decrease (possibly linear) towards or beyond z-score = −2; Phase 2. MD is still reduced but tends to increase towards the normal range (Figs. 3A and C). A third phase exists within a window of Barthel ~70 and below, in which MD is increasing but within the normal to low normal range and with a lower rate of change (Figs. 3A and C). MD values seem to have the same tendency across all brain lobes (Figs. 3B and D). In summary, it seems that MD tends to decrease in earlier stages of disease (Barthel 100 to ~85), then begins to increase rapidly and later more slowly towards normal or lower normal values starting from approximately Barthel 85 and below.

3.4. Thickness as function of Barthel score in cross-sectional and longitudinal analyses

When exploring the relationship between Barthel score and both cross-sectional measurements of cortical thickness/volume as well as the longitudinal changes in these values with splines, no clear pattern emerged. There was no discernible relationship between modified Barthel and thickness/volume and there was no change in thickness over two months (not shown).

4. Discussion

To our knowledge, this is the first study with complete cortical and subcortical GM quantification of MD both cross-sectionally and longitudinally in a cohort of sCJD subjects. In our cross-sectional analysis, decreased MD (restricted diffusion) was seen mostly in the temporal and parietal lobes and subcortical VOIs; no VOIs had increased MD.

Our longitudinal analysis surprisingly showed that there was a significant inverse correlation between Barthel and MD, as Barthel decreased or worsened, MD increased. Furthermore, using splines, we found a nonlinear relationship between either MD or change in MD and baseline Barthel score (an indication of the patient's clinical stage) (Fig. 3). This suggest a more complex – neither linear, nor unidirectional – model of MD changes over the disease course. The well-established and documented phase of decreased MD appears to be followed by a stage of increasing MD that is highly correlated with worsening of clinical function.

Table 2
Cross-sectional analysis of average gray matter mean diffusivity in sCJD compared to controls by whole brain and volumes of interest after correction for multiple comparisons.

Whole brain	Mean diffusivity[a] ($mm^2/s \times 10^{-3}$)	
	Controls	sCJD
Cortical GM	1041 ± 91	**945 ± 88*** **
Subcortical GM	913 ± 75	**830 ± 56*** **

VOIs	Mean diffusivity[a] ($mm^2/s \times 10^{-3}$)			
	Left hemisphere		Right hemisphere	
	Controls	sCJD	Controls	sCJD
Frontal				
Caudalmiddlefrontal	1070 ± 109	985 ± 111	1057 ± 136	949 ± 113(*)
Lateralorbitofrontal	1003 ± 96	946 ± 85	984 ± 77	908 ± 99(*)
Medialorbitofrontal	1057 ± 77	981 ± 112	1064 ± 97	**960 ± 112****
Parsopercularis	1137 ± 127	1064 ± 104	1097 ± 135	1013 ± 136
Paracentral	971 ± 139	891 ± 100	968 ± 108	918 ± 99
Parsorbitalis	1092 ± 134	1055 ± 168	1023 ± 85	949 ± 160
Parstriangularis	1134 ± 169	1089 ± 143	1074 ± 111	1005 ± 168
Precentral	1113 ± 126	1029 ± 91(*)	1092 ± 115	1016 ± 113
Rostralmiddlefrontal	1160 ± 136	1059 ± 141	1143 ± 149	1022 ± 155
Superiorfrontal	1075 ± 88	994 ± 105(*)	1060 ± 111	961 ± 101(*)
Frontalpole	1150 ± 139	1059 ± 229	1147 ± 147	1054 ± 259
Limbic				
Caudalanteriorcingulate	1078 ± 124	1006 ± 114	1048 ± 114	969 ± 111
Isthmuscingulate	950 ± 86	**835 ± 109****	972 ± 104	**823 ± 92****
Posteriorcingulate	951 ± 86	887 ± 92	974 ± 117	**857 ± 103****
Rostralanteriorcingulate	1023 ± 71	953 ± 98(*)	1005 ± 77	927 ± 109(*)
Insula	1061 ± 105	988 ± 104	1089 ± 103	993 ± 110(*)
Temporal				
Entorhinal	952 ± 63	920 ± 127	987 ± 89	935 ± 182
Fusiform	912 ± 78	**796 ± 107****	889 ± 59	**783 ± 126****
Inferiortemporal	925 ± 101	**801 ± 97*****	917 ± 103	**763 ± 107*****
Middletemporal	990 ± 104	**861 ± 103*****	978 ± 104	**821 ± 120*****
Temporalpole	1095 ± 184	1035 ± 107	1026 ± 89	1053 ± 197
Parahippocampal	1041 ± 67	**909 ± 114****	1011 ± 65	**872 ± 129****
Superiortemporal	1085 ± 104	1017 ± 127	1063 ± 107	989 ± 129
Transversetemporal	1123 ± 168	1065 ± 129	1101 ± 144	1079 ± 151
Bankssts	1015 ± 112	**858 ± 118****	974 ± 105	**838 ± 130****
Parietal				
Inferiorparietal	1038 ± 129	**873 ± 127****	1009 ± 101	**845 ± 136****
Postcentral	1153 ± 147	**1033 ± 103****	1123 ± 136	1038 ± 114(*)
Precuneus	990 ± 101	**840 ± 112****	1005 ± 81	**851 ± 121****
Superiorparietal	1084 ± 126	**949 ± 126****	1086 ± 116	**960 ± 149(*)**
Supramarginal	1084 ± 135	**931 ± 129****	1051 ± 118	**909 ± 132****
Occipital				
Cuneus	1051 ± 84	**936 ± 109****	1057 ± 74	940 ± 149(*)
Lateraloccipital	977 ± 101	874 ± 123(*)	973 ± 103	**839 ± 133****
Lingual	983 ± 92	915 ± 146	1017 ± 95	916 ± 132(*)
Pericalcarine	1089 ± 130	**990 ± 107****	1094 ± 136	**963 ± 132****
Subcortical GM				
Amygdala	933 ± 61	**858 ± 65****	931 ± 77	878 ± 66(*)
Caudate	925 ± 87	**822 ± 92****	952 ± 110	**834 ± 101****
Hippocampus	1107 ± 96	1047 ± 81	1083 ± 106	1032 ± 81
Pallidum	813 ± 76	**722 ± 67****	796 ± 82	**718 ± 59****
Putamen	807 ± 79	**719 ± 69****	810 ± 75	**705 ± 73****
Thalamus	896 ± 82	**815 ± 63****	901 ± 79	**814 ± 65****

Bold are statistically significant results of decreased MD between sCJD and controls. *** = areas with statistically significant reduced MD in sCJD compared to controls ($0.001 \leq p < 0.01$). ** = areas with statistically significant reduced MD in sCJD compared to controls ($0.01 \leq p < 0.05$); (*) = areas with trend of statistically significant reduced MD in sCJD compared to controls ($0.05 \leq p$ value < 0.1). No VOI had increased MD in sCJD compared to controls. GM = gray matter.

[a] Mean diffusivity values for whole brain cortical and subcortical gray matter and for single VOIs are reported in $mm^2/s \times 10^{-3}$ as average ± standard deviation for both control and sCJD groups.

4.1. Cross sectional analysis

Our results confirm prior non-quantitative assessments showing diffuse involvement of the GM in sCJD (Shiga et al., 2004; Tschampa et al., 2007; Vitali et al., 2011; Zerr et al., 2009). The pattern of involvement showed a relative increasing anterior to posterior gradient of restricted MD in the cortical GM, with less involvement of frontal and most limbic regions compared to temporal, parietal, posterior cingulate and to a lesser extent, occipital regions. Furthermore, all subcortical regions, except for the hippocampi, and right amygdala, had reduced MD after FDR.

4.2. Regional involvement and discordance between visual and quantified assessment

Whereas some visual assessment studies in sCJD have shown extensive frontal cortical involvement (Tschampa et al., 2007; Vitali et al., 2011; Young et al., 2005; Zerr et al., 2009), particularly in the superior

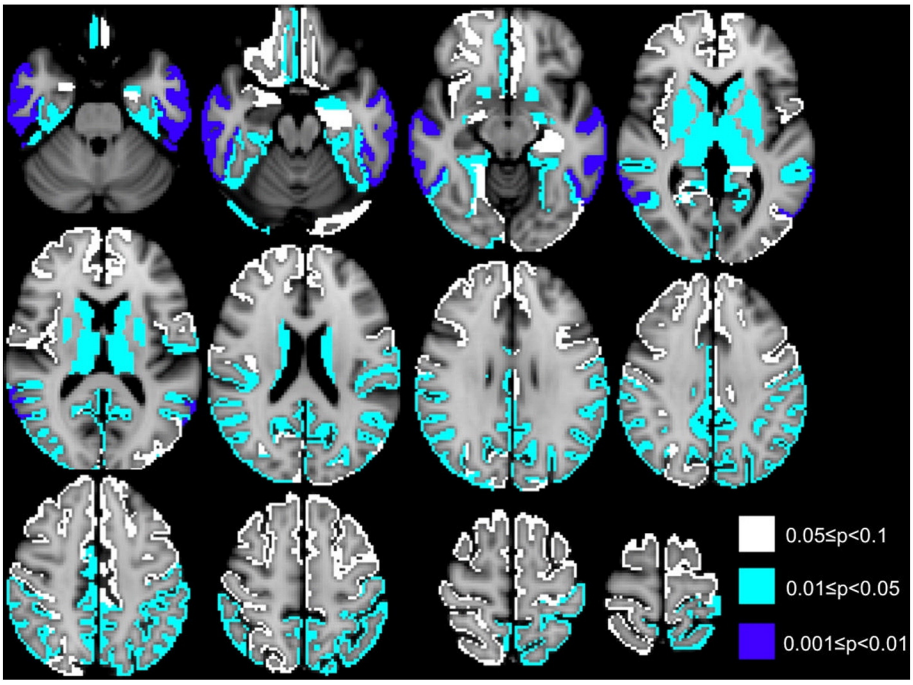

Fig. 1. Average mean diffusivity (MD) cross-sectionally in sCJD cohort versus controls per brain volumes of interest (VOIs) (after correction for multiple comparisons (FDR)). The colored areas are regions with significantly reduced (or a strong trend towards) mean MD in sCJD versus controls superposed on the Montreal Neurological Institute (MNI) atlas. White VOIs have a trend towards reduced average mean MD with p-values ≥0.05 and <0.1. Teal VOIs have significantly reduced average MD with p values ≥0.01 and <0.05. Blue VOIs have significantly reduced average MD with p values ≥0.001 and <0.01. Sporadic CJD had VOIs with reduced average MD compared to controls primarily in temporal and parietal lobes and deep nuclei. No VOI had increased MD in sCJD compared to controls. Orientation is radiologic (right brain is left side of image).

frontal gyrus (Tschampa et al., 2007; Vitali et al., 2011; Young et al., 2005), we only found a trend towards frontal cortical involvement (Fig. 1). Zerr et al. found on visual assessment that many non-CJD controls had frontal cortical hyperintensities that were misread as consistent with CJD and thus frontal regions could not reliably distinguish sCJD from controls (Zerr et al., 2009). The relative lack of frontal and

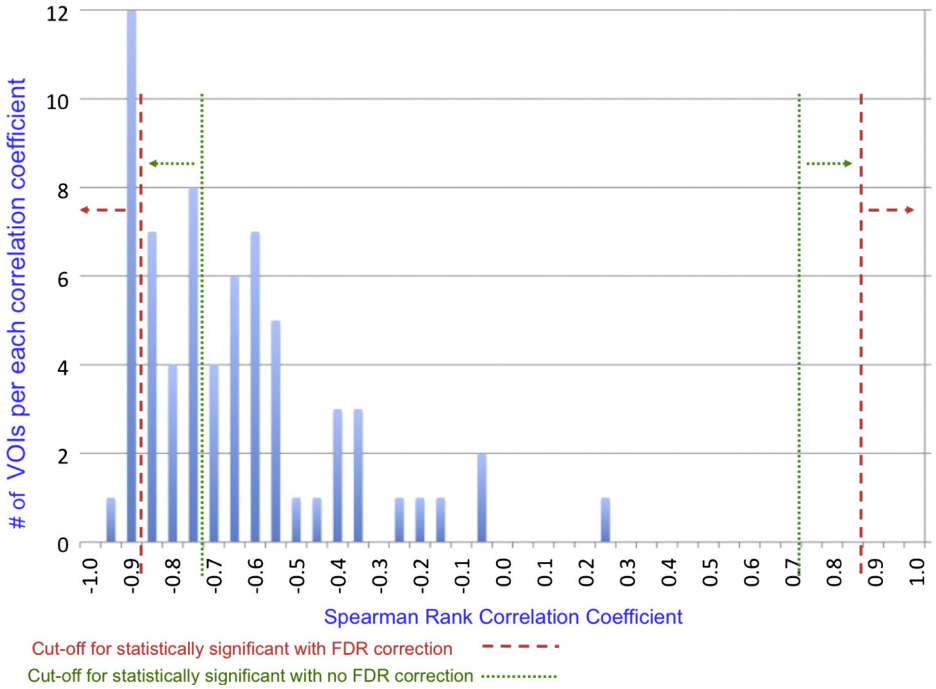

Fig. 2. Inverse correlation of change in Barthel and change in MD over two months. Distribution of Spearman Rank Correlation Coefficients of change in the modified Barthel and average MD over two months for all cortical VOIs. The graph shows the number of cortical VOIs (y axis) per each Spearman Rank Correlation Coefficient (x axis: values from 1 to −1). The green dotted line shows the limit for statistically significant values without FDR; the red dash line shows the limit for statistically significant values with FDR. At whole brain, hemispheric, lobar and the VOI level, all areas (except the right parahippocampus) showed an inverse (negative) relationship between the change in the (delta) modified Barthel and the change in the (delta) average MD with 15 VOIs (13 cortical and 2 subcortical; outside red dotted line) reaching statistical significance with FDR ($p < 0.05$)—as modified Barthel decreased/worsened, MD increased. For many brain VOIs, there was at least a trend towards increased MD with worsening modified Barthel.

anterior and mid-limbic involvement on our quantitative cross-sectional analysis is in contrast to our, and others', clinical experience, in which there was clear involvement on DWI and ADC sequences in these regions (Tschampa et al., 2007; Vitali et al., 2011; Young et al., 2005). We discuss below why this might be the case.

We partly confirm sparing of the peri-Rolandic cortex noted previously (Lin et al., 2006; Young et al., 2005); here we found, on average, sparing of primary motor and much of the right primary somatosensory cortices, but involvement of the left post-central gyrus. Lin et al. suggested that this relative sparing of the Rolandic cortex by visual assessment might be due to concurrent iron-related hypointensity (so called T2 black-out effect) (Lin et al., 2006). Our data, however, suggested against this because quantitative MD assessment should overcome the possible T2 black-out effect (as there is no evidence that iron content affects diffusivity) and we found relative sparing of this region (Supplemental data). Therefore, other factors are necessary to explain the relative sparing of this area on DWI.

Although the cingulate and insula are usually bright on visual assessment in sCJD (Tschampa et al., 2007; Vitali et al., 2011), on our quantitative assessment these regions generally only trended towards significant involvement; only the isthmus cingulate and right posterior cingulate survived FDR. The cingulate and insula are known to be areas of DWI/FLAIR hyperintensity even in healthy subjects (Asao et al., 2008), however, which might lead to false-positive readings in non-CJD and false-negatives in sCJD (Zerr et al., 2009). Using the ADC map should help identify true abnormalities in these regions (Asao et al., 2008; Vitali et al., 2011). Mesial-temporal involvement often also is difficult to interpret on DWI due to artifact (Tschampa et al., 2007; Zerr et al., 2009). In a prior, visual assessment study, we read the hippocampus/amygdala as one structure and reported involvement (Vitali et al., 2011), whereas here quantitatively we found involvement of the amygdala, but not the hippocampus.

Corroborating several prior visual assessment papers, we found relatively extensive subcortical involvement and partial occipital involvement (Tschampa et al., 2007; Vitali et al., 2011; Young et al., 2005). A recent paper focusing on the role of MRI, CSF and EEG in the diagnosis of sCJD versus healthy controls and non-prion rapidly progressive dementias examined quantitatively 10 mm spherical ROIs in gray (precuneus, frontal cortex, pulvinar and caudate head) and white (posterior limb of the internal capsule and corpus callosum) matter regions of nine sCJD subjects and found decreased MD in the caudate and pulvinar ROIs, and no FA abnormalities (Wang et al., 2013). Despite it being a more limited study in terms of regions analyzed and the number of subjects, it partially supports our cross-sectional findings, although we found more extensive reduced MD. Similarly to Wang et al., we confirm in a more neuroanatomically extensive analysis the

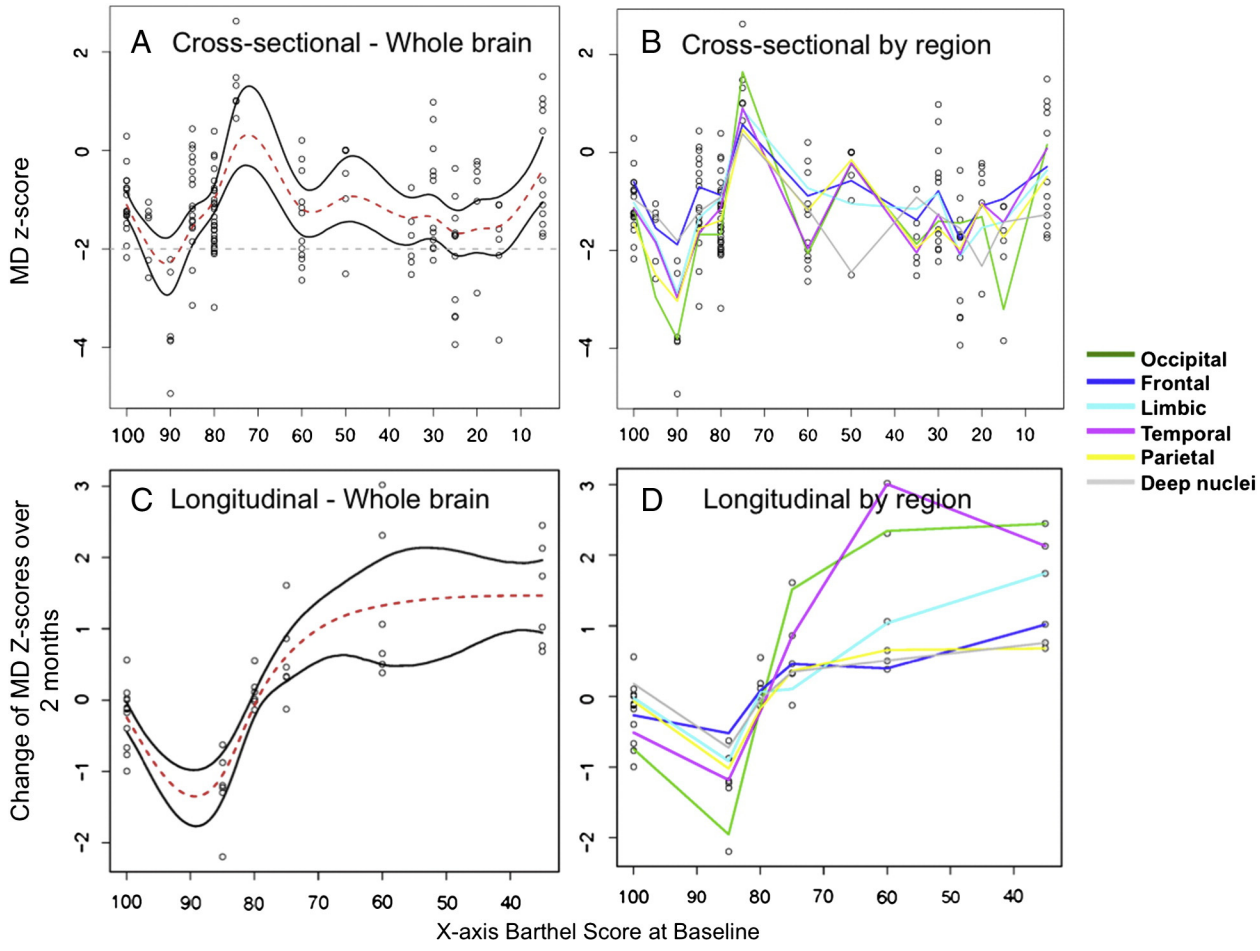

Fig. 3. Cross-sectional and longitudinal (change) in Mean Diffusivity in sCJD vs. Barthel score. (A–B) Cross-sectional data. Using splines, we estimated group-wise average MD values at (A) whole brain and (B) at lobar/region level (frontal, limbic, temporal, parietal, occipital, deep nuclei), as a function of baseline modified Barthel scores for the 26 sCJD subjects. Circles in the figures represent average of MD values within each lobe/region for each subject studied either cross-sectionally (A–B) or longitudinally (C–D). In A, we show the 95% confidence interval (black solid lines) and estimate of average tendency in MD (red dotted line). In B, we show estimates of average tendency in MD at lobar levels (colored solid lines). (C–D) Longitudinal data. The average change over 2 months in MD in seven sCJD subjects in (C) whole brain and (D) in each lobes/region independently (frontal, limbic, temporal, parietal, occipital, deep nuclei) as a function of baseline Barthel score was estimated using splines. In C, we show the 95% confidence interval (black solid lines) and estimate of average tendency in change of MD (red dotted line). In D, we show estimates of average tendency in change of MD at the lobar level (colored solid lines). We obtained an identical graph to Fig. 3A even by excluding 7 patients with longitudinal scans (not shown). Deep nuclei = thalamus, pallidum, caudate and putamen; limbic lobe = cingulate cortex and insula.

absence of any FA change in the cortical or subcortical gray matter of sCJD compared to controls.

Involvement of the GP is uncommonly reported in sCJD on MRI (Shiga et al., 2004; Tschampa et al., 2007; Vitali et al., 2011; Young et al., 2005). In our prior visual assessment, we often found decreased ADC in the GP often without concomitant DWI hyperintensity (Vitali et al., 2011). In this current analysis, quantitatively we found restricted MD in bilateral GP, supporting our previous ADC finding. The relative lack of GP involvement on DWI/FLAIR might be from the high iron deposition in the GP causing a T2 black-out effect on visual assessment (Lin et al., 2006; Schenker et al., 1993; Vitali et al., 2011).

Contrary to previous observations of T1 hyperintensity in certain deep nuclei structures, particularly the GP (de Priester et al., 1999; Vitali et al., 2011), in this study, T1 relaxometry did not show any differences between our sCJD cohort and controls in any regions, including the GP. This might be because T1 hyperintensity has only been reported in a few sCJD patients and our study was at group-wise level.

4.3. Comparison of mean MD on a lobar level across sCJD based on prion type or codon 129 polymorphism

MRI pattern differences within sCJD molecular subtypes (based on both prion typing and codon 129 polymorphism) (Parchi et al., 1999) described by Meissner et al. (Meissner et al., 2009) require updating for several reasons. Qualitatively assessment of real pattern of involvement in sCJD is problematic, especially when using different scanners and MRI sequences. Moreover, sCJD subtype classification has evolved due to many cases with concomitant presence of prion types 1 and 2 (Polymenidou et al., 2005; Puoti et al., 2012). Finally, the pattern of involvement likely evolves in the course of the disease (see Section "4.5 MD changes over time" below). Due to the small number of patients in this study, it was not possible for us to compare all sCJD molecular subtypes. Nevertheless, our regression analysis based on either prion type or codon 129 polymorphism (correcting for disease stage based on Barthel) showed differences based on these two factors. Subjects with type 1 prions had more reduced cortical average MD than those with type 2 prions in several lobes bilaterally. Furthermore, codon 129 VV cases showed more reduced MD in the deep nuclei compared to MM cases. These findings need to be explored in a larger cohort.

4.4. Atrophy and MD

No cortical or subcortical regions showed any atrophy relative to controls. Clinically, on serial visual assessment, however, we note significant atrophy in sCJD patients with prolonged survival, typically a year or longer, but often after just several months. Atrophy might not have been detected in this analysis for several reasons, including group-wise averaging might have prevented detection of atrophy, Freesurfer might not have been sufficiently sensitive particularly with 1.5 T scans, and/or atrophy might occur at later stages of disease. Larger serial studies, on stronger magnets, such as 3 T, might be required to determine the extent and rate of atrophy in sCJD. Not surprisingly, we also found no correlation of MD with either thickness/volume. This might also be because reduced MD in prion disease is associated with vacuolation, prion deposition and possibly gliosis (Geschwind et al., 2009; Manners et al., 2009). Atrophy, however, is characterized by increased MD values (Chua et al., 2009; Whitwell et al., 2010).

4.5. MD changes over time

Our longitudinal group-wise analysis suggested increasing MD in most brain regions over two months, with only a few regions suggesting slightly reducing diffusion. Moreover, there was a strong inverse correlation between the change in clinical function (modified Barthel index) and MD—as clinical function worsened, MD increased (Fig. 2 and Supplemental Table 1). Although restricted MD is a well documented finding and strong diagnostic marker for sCJD (Shiga et al., 2004; Vitali et al., 2011; Zerr et al., 2009), surprisingly our data suggests that in the course of the disease this MD change is not unidirectional, decreasing early and later becoming less reduced.

This finding, however, might be consistent with some prior findings in human prion disease. Hyare et al. found that in genetic prion disease, increasing whole GM mean MD was an independent predictor of worsening CDR, Barthel and Rankin scales (Hyare et al., 2010). Our findings also are consistent with literature showing that regions with initially restricted diffusion might show disappearance of this restricted diffusion, consistent with increasing MD, particularly in patients with prolonged prion disease (Hirose et al., 1998; Matoba et al., 2001; Tschampa et al., 2003; Ukisu et al., 2005). Therefore, decreasing MD in sCJD in earlier affected regions might arrest and possibly reverse with progressive increasing MD towards normalization ("relative normalization") and even increased MD (Fig. 3) (Fulbright et al., 2006; Haik et al., 2008; Hirose et al., 1998). Importantly for consideration of future treatment trials, our data suggests that the increasing MD phase is associated with the more dramatic loss of function (Fig. 3) and might represent a late, and possibly even irreversible, phase of disease.

As noted previously, different stages of disease are probably co-occurring in the same brain (Haik et al., 2008; Hirose et al., 1998). Because many of our cases in this analysis were not very early stage, we suspect less involvement of frontal and limbic regions in this cross-sectional analysis is due to these frontal/limbic regions having been affected earlier in the disease course and might have already gone through the phase of decreasing MD and be at the stage of increasing or "relative normalization of" MD.

The relative normalization of MD in the middle to late stages of the disease might be due to underlying histopathological changes. The later stages of sCJD are characterized by neuronal loss and gliosis (Kretzschmar et al., 1996; Ukisu et al., 2005). Severe brain atrophy in late stage CJD correlates with the disappearance of previous hyperintense DWI signal, (Hirose et al., 1998; Matoba et al., 2001; Tribl et al., 2002), probably due to increasing MD values. Therefore, neuronal loss and/or gliosis might allow increased water flow and augmentation of MD values in regions in late disease stages (Tschampa et al., 2003). This is consistent with increased MD seen in other neurodegenerative diseases, (Chua et al., 2009; Kantarci et al., 2010; Oreja-Guevara et al., 2005; Whitwell et al., 2010) as well as genetic prion disease (Cohen et al., 2009), which probably due to progression of neuronal loss (and/or gliosis). Interestingly, in a single case of fatal familial insomnia, with MRI four days prior to death, increased MD values appeared to correlate with gliosis but not PrP^{Sc} deposition (Haik et al., 2008). It is not clear why gliosis might cause increased MD; some literature suggests otherwise (Pfefferbaum et al., 2010), and we could predict that isolated gliosis (not associated with neuronal loss) would cause a reduced diffusion of water molecules by adding a barrier. Furthermore, as gliosis and neuronal loss often are highly correlated in prion disease (Manners et al., 2009), and many studies assess gliosis neuropathologically without accounting for neuronal loss, it might be that increased MD actually is due to neuronal loss, not gliosis. Additionally, the increased size of vacuoles and their coalescence in late stage of CJD also might be expected to cause an increased diffusion of free water molecules (Geschwind et al., 2009).

4.6. Clinical correlation with MRI metrics

The lack of correlation between clinical scales (Barthel, NPI, and MMSE) and gray matter MRI values cross-sectionally might be due to several reasons. As we did not find a significant difference in thickness/volume in our groupwise analysis of sCJD versus controls, there might have not been sufficient atrophy in individual subjects to correlate with clinical scales. In sCJD, there is often not appreciable atrophy except in late stages of patients with prolonged disease courses.

In retrospect, knowing that the course of MD changes appear to be non-linear and non-unidirectional (i.e., J-shaped curve) it makes sense that these scales that are unidirectional and generally linear in this disease might not correlate with MD cross-sectionally or longitudinally. The individual variability in clinical phenotype of sCJD patients would likely result in great variations in the NPI and MMSE, further explaining the lack of correlation of these measures with MD. As noted in the Results section, however, we found that the Barthel correlated with longitudinal MD changes in several brain regions. This is not unexpected as we and others have found that ADL scales, such as the Barthel, track CJD progression far better than neuropsychometric measures (Geschwind et al., 2013; Mead et al., 2011). Contrary to what we had expected, however, the correlation between Barthel and MD changes was inverse, as Barthel was decreasing, MD tends to increase. Our longitudinal data seems to suggest that a steeper decline in function (i.e., Barthel) occurs at a middle-late stage of disease, once the MD values start to increase towards a relative normalization of values (Fig. 3). This finding needs to be studied in a larger cohort.

5. Conclusion

Our findings show that MRI is not only important for sCJD diagnosis, but also for studying the underlying pathophysiology of prion disease. This study provides insight into the evolution of MRI changes in sCJD, suggesting a model for pathological progression of human prion disease. If our hypothesis of later stage normalization of MD is correct, it would be difficult to use MD values in isolation to monitor sCJD progression in future treatment trials, as one might not know at which point on a U or J shaped curve the region is moving towards decreasing versus increasing MD. Serial MD values, however, might inform whether the MD values are decreasing or increasing. Additionally, inclusion of other MRI findings, such as T2-quantification or atrophy, might help determine a patient's disease stage. Lastly, the recent evidence for a prion-like spread for other neurodegenerative dementias (Prusiner, 2012; Raj et al., 2012) has highlighted the need for better understanding disease spread in sCJD. Larger longitudinal studies are needed to confirm our model of MD changes over the course of the disease.

One limitation of this study was that the limited number of controls made it not possible to obtain normal threshold values to assess diffusion changes at single subject levels. Future studies applying similar methodologies at a single subject level might be able to show better the correlation between diffusion changes and atrophy, as well as possible differences in between the different sCJD molecular subtypes.

Supplementary data to this article can be found online at http://dx.doi.org/10.1016/j.nicl.2014.01.011.

Acknowledgments

The authors thank referring physicians; the U.S. National Prion Disease Pathology Surveillance Center (NPDPSC) for assistance with *PRNP* analyses, prion typing and pathological analyses; Henry Sanchez, MD for pathological analyses; the U.S. CJD Foundation (for supporting our patients and families), and to our patients and their families.

References

Alperovitch, A., Zerr, I., Pocchiari, M., Mitrova, E., de Pedro Cuesta, J., Hegyi, I., Collins, S., Kretzschmar, H., van Duijn, C., Will, R.G., 1999. Codon 129 prion protein genotype and sporadic Creutzfeldt–Jakob disease. Lancet 353, 1673–1674.

Andrews, N.J., 2010. Incidence of variant Creutzfeldt–Jakob disease diagnoses and deaths in the UK January 1994–December 2009. Statistics Unit, Centre for Infections, Health Protection Agency, London.

Asao, C., Hirai, T., Yoshimatsu, S., Matsukawa, T., Imuta, M., Sagara, K., Yamashita, Y., 2008. Human cerebral cortices: signal variation on diffusion-weighted MR imaging. Neuroradiology 50, 205–211.

Cali, I., Castellani, R., Alshekhlee, A., Cohen, Y., Blevins, J., Yuan, J., Langeveld, J.P., Parchi, P., Safar, J.G., Zou, W.Q., Gambetti, P., 2009. Co-existence of scrapie prion protein types 1 and 2 in sporadic Creutzfeldt–Jakob disease: its effect on the phenotype and prion-type characteristics. Brain 132, 2643–2658.

Chua, T.C., Wen, W., Chen, X., Kochan, N., Slavin, M.J., Trollor, J.N., Brodaty, H., Sachdev, P.S., 2009. Diffusion tensor imaging of the posterior cingulate is a useful biomarker of mild cognitive impairment. Am. J. Geriatr. Psychiatry 17, 602–613.

Cohen, O.S., Hoffmann, C., Lee, H., Chapman, J., Fulbright, R.K., Prohovnik, I., 2009. MRI detection of the cerebellar syndrome in Creutzfeldt–Jakob disease. Cerebellum 8, 373–381.

Cummings, J.L., 1997. The Neuropsychiatric Inventory: assessing psychopathology in dementia patients. Neurology 48, S10–S16.

Dale, A.M., Fischl, B., Sereno, M.I., 1999. Cortical surface-based analysis. I. Segmentation and surface reconstruction. Neuroimage 9, 179–194.

de Priester, J.A., Jansen, G.H., de Kruijk, J.R., Wilmink, J.T., 1999. New MRI findings in Creutzfeldt–Jakob disease: high signal in the globus pallidus on T1-weighted images. Neuroradiology 41, 265–268.

Desikan, R.S., Segonne, F., Fischl, B., Quinn, B.T., Dickerson, B.C., Blacker, D., Buckner, R.L., Dale, A.M., Maguire, R.P., Hyman, B.T., Albert, M.S., Killiany, R.J., 2006. An automated labeling system for subdividing the human cerebral cortex on MRI scans into gyral based regions of interest. Neuroimage 31, 968–980.

Driscoll, I., Davatzikos, C., An, Y., Wu, X., Shen, D., Kraut, M., Resnick, S.M., 2009. Longitudinal pattern of regional brain volume change differentiates normal aging from MCI. Neurology 72, 1906–1913.

Efron, B., Tibshirani, R.J., 1993. An Introduction to the Bootstrap, Chapter 10. Chapman and Hall, New York.

Fischl, B., Sereno, M.I., Dale, A.M., 1999. Cortical surface-based analysis. II: inflation, flattening, and a surface-based coordinate system. Neuroimage 9, 195–207.

Fischl, B., van der Kouwe, A., Destrieux, C., Halgren, E., Segonne, F., Salat, D.H., Busa, E., Seidman, L.J., Goldstein, J., Kennedy, D., Caviness, V., Makris, N., Rosen, B., Dale, A.M., 2004. Automatically parcellating the human cerebral cortex. Cereb. Cortex 14, 11–22.

Fulbright, R.K., Kingsley, P.B., Guo, X., Hoffmann, C., Kahana, E., Chapman, J.C., Prohovnik, I., 2006. The imaging appearance of Creutzfeldt–Jakob disease caused by the E200K mutation. Magn. Reson. Imaging 24, 1121–1129.

Geschwind, M.D., Josephs, K.A., Parisi, J.E., Keegan, B.M., 2007. A 54-year-old man with slowness of movement and confusion. Neurology 69, 1881–1887.

Geschwind, M.D., Potter, C.A., Sattavat, M., Garcia, P.A., Rosen, H.J., Miller, B.L., DeArmond, S.J., 2009. Correlating DWI MRI with pathologic and other features of Jakob–Creutzfeldt disease. Alzheimer Dis. Assoc. Disord. 23, 82–87.

Geschwind, M.D., Kuo, A.L., Wong, K.S., Haman, A., Devereux, G., Raudabaugh, B.J., Johnson, D.Y., Torres-Chae, C.C., Finley, R., Garcia, P., Thai, J.N., Cheng, H.Q., Neuhaus, J.M., Forner, S.A., Duncan, J.L., Possin, K.L., DeArmond, S.J., Prusiner, S.B., Miller, B.L., 2013. Quinacrine treatment trial for sporadic Creutzfeldt–Jakob disease. Neurology 81, 2015–2023.

Green, P.J., Silverman, B.W., 1994. Nonparametric Regression and Generalized Linear Models: A Roughness Penalty Approach, 1st ed. Chapman & Hall, London; New York.

Haik, S., Galanaud, D., Linguraru, M.G., Peoc'h, K., Privat, N., Faucheux, B.A., Ayache, N., Hauw, J.J., Dormont, D., Brandel, J.P., 2008. In vivo detection of thalamic gliosis: a pathoradiologic demonstration in familial fatal insomnia. Arch. Neurol. 65, 545–549.

Hirose, Y., Mokuno, K., Abe, Y., Sobue, G., Matsukawa, N., 1998. A case of clinically diagnosed Creutzfeldt–Jakob disease with serial MRI diffusion weighted images. Rinsho Shinkeigaku 38, 779–782.

Hyare, H., Wroe, S., Siddique, D., Webb, T., Fox, N.C., Stevens, J., Collinge, J., Yousry, T., Thornton, J.S., 2010. Brain-water diffusion coefficients reflect the severity of inherited prion disease. Neurology 74, 658–665.

Kantarci, K., Avula, R., Senjem, M.L., Samikoglu, A.R., Zhang, B., Weigand, S.D., Przybelski, S.A., Edmonson, H.A., Vemuri, P., Knopman, D.S., Ferman, T.J., Boeve, B.F., Petersen, R.C., Jack Jr., C.R., 2010. Dementia with Lewy bodies and Alzheimer disease: neurodegenerative patterns characterized by DTI. Neurology 74, 1814–1821.

Kono, S., Manabe, Y., Fujii, D., Sakai, Y., Narai, H., Omori, N., Kitamoto, T., Abe, K., 2011. Serial diffusion-weighted MRI and SPECT findings in a Creutzfeldt–Jakob disease patient with V180I mutation. J. Neurol. Sci. 301, 100–103.

Kretzschmar, H.A., Ironside, J.W., DeArmond, S.J., Tateishi, J., 1996. Diagnostic criteria for sporadic Creutzfeldt–Jakob disease. Arch. Neurol. 53, 913–920.

Lee, H., Cohen, O.S., Rosenmann, H., Hoffmann, C., Kingsley, P.B., Korczyn, A.D., Chapman, J., Prohovnik, I., 2012. Cerebral white matter disruption in Creutzfeldt–Jakob disease. AJNR Am. J. Neuroradiol. 33, 1945–1950.

Lin, Y.R., Young, G.S., Chen, N.K., Dillon, W.P., Wong, S., 2006. Creutzfeldt–Jakob disease involvement of rolandic cortex: a quantitative apparent diffusion coefficient evaluation. AJNR Am. J. Neuroradiol. 27, 1755–1759.

Manners, D.N., Parchi, P., Tonon, C., Capellari, S., Strammiello, R., Testa, C., Tani, G., Malucelli, E., Spagnolo, C., Cortelli, P., Montagna, P., Lodi, R., Barbiroli, B., 2009. Pathologic correlates of diffusion MRI changes in Creutzfeldt–Jakob disease. Neurology 72, 1425–1431.

Matoba, M., Tonami, H., Miyaji, H., Yokota, H., Yamamoto, I., 2001. Creutzfeldt–Jakob disease: serial changes on diffusion-weighted MRI. J. Comput. Assist. Tomogr. 25, 274–277.

Mead, S., Ranopa, M., Gopalakrishnan, G.S., Thompson, A.G., Rudge, P., Wroe, S., Kennedy, A., Hudson, F., MacKay, A., Darbyshire, J.H., Collinge, J., Walker, A.S., 2011. PRION-1 scales analysis supports use of functional outcome measures in prion disease. Neurology 77, 1674–1683.

Meissner, B., Kallenberg, K., Sanchez-Juan, P., Collie, D., Summers, D.M., Almonti, S., Collins, S.J., Smith, P., Cras, P., Jansen, G.H., Brandel, J.P., Coulthart, M.B., Roberts, H., Van Everbroeck, B., Galanaud, D., Mellina, V., Will, R.G., Zerr, I., 2009. MRI lesion profiles in sporadic Creutzfeldt–Jakob disease. Neurology 72, 1994–2001.

Oreja-Guevara, C., Rovaris, M., Iannucci, G., Valsasina, P., Caputo, D., Cavarretta, R., Sormani, M.P., Ferrante, P., Comi, G., Filippi, M., 2005. Progressive gray matter damage

in patients with relapsing-remitting multiple sclerosis: a longitudinal diffusion tensor magnetic resonance imaging study. Arch. Neurol. 62, 578–584.
Parchi, P., Giese, A., Capellari, S., Brown, P., Schulz-Schaeffer, W., Windl, O., Zerr, I., Budka, H., Kopp, N., Piccardo, P., Poser, S., Rojiani, A., Streichemberger, N., Julien, J., Vital, C., Ghetti, B., Gambetti, P., Kretzschmar, H., 1999. Classification of sporadic Creutzfeldt–Jakob disease based on molecular and phenotypic analysis of 300 subjects. Ann. Neurol. 46, 224–233.
Pfefferbaum, A., Adalsteinsson, E., Rohlfing, T., Sullivan, E.V., 2010. Diffusion tensor imaging of deep gray matter brain structures: effects of age and iron concentration. Neurobiol. Aging 31, 482–493.
Polymenidou, M., Stoeck, K., Glatzel, M., Vey, M., Bellon, A., Aguzzi, A., 2005. Coexistence of multiple PrPSc types in individuals with Creutzfeldt–Jakob disease. Lancet Neurol. 4, 805–814.
Prusiner, S.B., 2012. Cell biology. A unifying role for prions in neurodegenerative diseases. Science 336, 1511–1513.
Puoti, G., Bizzi, A., Forloni, G., Safar, J.G., Tagliavini, F., Gambetti, P., 2012. Sporadic human prion diseases: molecular insights and diagnosis. Lancet Neurol. 11, 618–628.
R Core Team, 2013. A Language and Environment for Statistical Computing. R Foundation for Statistical Computing, Vienna, Austria.
Raj, A., Kuceyeski, A., Weiner, M., 2012. A network diffusion model of disease progression in dementia. Neuron 73, 1204–1215.
Schenker, C., Meier, D., Wichmann, W., Boesiger, P., Valavanis, A., 1993. Age distribution and iron dependency of the T2 relaxation time in the globus pallidus and putamen. Neuroradiology 35, 119–124.
Shiga, Y., Miyazawa, K., Sato, S., Fukushima, R.S., Shibuya, S., Sato, Y., Konno, H., Doh-ura, K., Mugikura, S., Tamura, H., Higano, S., Takahashi, S., Itoyama, Y., 2004. Diffusion-weighted MRI abnormalities as an early diagnostic marker for Creutzfeldt–Jakob disease. Neurology I63, 443–449.
Tribl, G.G., Strasser, G., Zeitlhofer, J., Asenbaum, S., Jarius, C., Wessely, P., Prayer, D., 2002. Sequential MRI in a case of Creutzfeldt–Jakob disease. Neuroradiology 44, 223–226.
Tschampa, H.J., Murtz, P., Flacke, S., Paus, S., Schild, H.H., Urbach, H., 2003. Thalamic involvement in sporadic Creutzfeldt–Jakob disease: a diffusion-weighted MR imaging study. AJNR Am. J. Neuroradiol. 24, 908–915.
Tschampa, H.J., Kallenberg, K., Kretzschmar, H.A., Meissner, B., Knauth, M., Urbach, H., Zerr, I., 2007. Pattern of cortical changes in sporadic Creutzfeldt–Jakob disease. AJNR Am. J. Neuroradiol. 28, 1114–1118.
Ukisu, R., Kushihashi, T., Kitanosono, T., Fujisawa, H., Takenaka, H., Ohgiya, Y., Gokan, T., Munechika, H., 2005. Serial diffusion-weighted MRI of Creutzfeldt–Jakob disease. Am. J. Roentgenol. 184, 560–566.
Vitali, P., Maccagnano, E., Caverzasi, E., Henry, R.G., Haman, A., Torres-Chae, C., Johnson, D.Y., Miller, B.L., Geschwind, M.D., 2011. Diffusion-weighted MRI hyperintensity patterns differentiate CJD from other rapid dementias. Neurology 76, 1711–1719.
Wang, L.H., Bucelli, R.C., Patrick, E., Rajderkar, D., Alvarez Iii, E., Lim, M.M., Debruin, G., Sharma, V., Dahiya, S., Schmidt, R.E., Benzinger, T.S., Ward, B.A., Ances, B.M., 2013. Role of magnetic resonance imaging, cerebrospinal fluid, and electroencephalogram in diagnosis of sporadic Creutzfeldt–Jakob disease. J. Neurol. 260, 498–506.
White, A.R., Enever, P., Tayebi, M., Mushens, R., Linehan, J., Brandner, S., Anstee, D., Collinge, J., Hawke, S., 2003. Monoclonal antibodies inhibit prion replication and delay the development of prion disease. Nature 422, 80–83.
Whitwell, J.L., Avula, R., Senjem, M.L., Kantarci, K., Weigand, S.D., Samikoglu, A., Edmonson, H.A., Vemuri, P., Knopman, D.S., Boeve, B.F., Petersen, R.C., Josephs, K.A., Jack Jr., C.R., 2010. Gray and white matter water diffusion in the syndromic variants of frontotemporal dementia. Neurology 74, 1279–1287.
WHO, 1998. Global surveillance, diagnosis and therapy of human transmissible spongiform encephalopathies: Report of a WHO consultation Geneva, Switzerland 9–11 February 1998. World Health Organization: emerging and other communicable diseases, surveillance and controlWorld Health Organization, Geneva, Switzerland.
Young, G.S., Geschwind, M.D., Fischbein, N.J., Martindale, J.L., Henry, R.G., Liu, S., Lu, Y., Wong, S., Liu, H., Miller, B.L., Dillon, W.P., 2005. Diffusion-weighted and fluid-attenuated inversion recovery imaging in Creutzfeldt–Jakob disease: high sensitivity and specificity for diagnosis. AJNR Am. J. Neuroradiol. 26, 1551–1562.
Zerr, I., Kallenberg, K., Summers, D.M., Romero, C., Taratuto, A., Heinemann, U., Breithaupt, M., Varges, D., Meissner, B., Ladogana, A., Schuur, M., Haik, S., Collins, S.J., Jansen, G.H., Stokin, G.B., Pimentel, J., Hewer, E., Collie, D., Smith, P., Roberts, H., Brandel, J.P., van Duijn, C., Pocchiari, M., Begue, C., Cras, P., Will, R.G., Sanchez-Juan, P., 2009. Updated clinical diagnostic criteria for sporadic Creutzfeldt–Jakob disease. Brain 132, 2659–2668.